

Bose-Einstein Condensate in a Uniform Light-Induced Vector Potential

Y.-J. Lin, R. L. Compton, A. R. Perry, W. D. Phillips, J. V. Porto, and I. B. Spielman*

Joint Quantum Institute, National Institute of Standards and Technology, and University of Maryland, Gaithersburg, Maryland, 20899, USA

(Received 17 September 2008; published 30 March 2009)

We use a two-photon dressing field to create an effective vector gauge potential for Bose-Einstein-condensed ^{87}Rb atoms in the $F = 1$ hyperfine ground state. These Raman-dressed states are spin and momentum superpositions, and we adiabatically load the atoms into the lowest energy dressed state. The effective Hamiltonian of these neutral atoms is like that of charged particles in a uniform magnetic vector potential whose magnitude is set by the strength and detuning of the Raman coupling. The spin and momentum decomposition of the dressed states reveals the strength of the effective vector potential, and our measurements agree quantitatively with a simple single-particle model. While the uniform effective vector potential described here corresponds to zero magnetic field, our technique can be extended to nonuniform vector potentials, giving nonzero effective magnetic fields.

DOI: 10.1103/PhysRevLett.102.130401

PACS numbers: 03.75.Lm, 67.85.Hj

Ultracold atoms are an appealing system for the study of many-body correlated states relevant to condensed matter physics. These widely tunable, and nearly disorder-free systems have already realized one-dimensional Tonks-Girardeau gases [1], and the superfluid to Mott-insulator transition of a Bose-Einstein condensate (BEC) in an optical lattice [2]. The implementation of these simple iconic condensed matter systems paves the way for more interesting systems with exotic correlations and excitations, as in the fractional quantum Hall effect (FQHE) of a two-dimensional electron system in a strong magnetic field [3]. Simulating these systems with neutral atoms requires an effective Lorentz force, associated with a vector gauge potential. Current experimental approaches involve rotation of trapped BECs [4,5], where low field effects, such as the formation of an Abrikosov vortex lattice, have been observed. For technical reasons, this approach is limited to modest effective fields, too small for FQHE physics [5,6]. Most recent proposals to create significantly larger effective magnetic fields without rotation [7–10] involve optical coupling between internal atomic states, where the atoms are dressed in a spatially dependent manner. The effective magnetic field in such light-induced gauge potentials can be understood as a consequence of changing into a spatially varying basis of internal states. Even absent spatial gradients, light-induced gauge potentials can lead to remarkable physical effects such as an anisotropic Bogoliubov excitation spectrum [10], double well structures in the free-particle dispersion relation [11] (which we observe), and the spin-Hall effect in ultracold atoms [9].

Here we report the first observation of light-induced vector gauge potentials, produced by dressing a BEC with two counterpropagating Raman laser beams. The Raman beams couple internal (spin) states with linear momenta differing by twice the photon momentum. This gives rise to a spatial gradient of the phase difference

between spin components of the dressed state. As we will show, this spatially varying state leads to a nonzero vector potential when the coupling is detuned from Raman resonance. We adiabatically load the BEC into the dressed state, and measure properties of the dressed-state dispersion relation by probing its spin and momentum decomposition. While the atoms are stationary in the lab frame (i.e., zero group velocity), the momenta of the individual spin components of the dressed state show a nonzero phase velocity depending on the strength and detuning of the Raman coupling. Our measurements agree with a single-particle model, and demonstrate the presence of an effective vector potential.

We dress a ^{87}Rb BEC in the $F = 1$ ground state with two Raman laser beams counterpropagating along \hat{x} . These beams couple states $|m_F, k_x\rangle$ differing in internal angular momentum by \hbar ($\Delta m_F = \pm 1$), and differing in linear momentum $\hbar k_x$ by $2\hbar k_r$. Here, $\hbar k_r = h/\lambda$ is the single-photon recoil momentum, and λ is the wavelength of the Raman beams. We define $E_r = \hbar^2 k_r^2/2m$ as the recoil energy. The family of three states coupled by the Raman field, $\Psi(\tilde{k}_x) = \{|-1, \tilde{k}_x + 2k_r\rangle, |0, \tilde{k}_x\rangle, |+1, \tilde{k}_x - 2k_r\rangle\}$, is labeled by the wave vector of the quasimomentum, \tilde{k}_x . The Raman beams have frequencies ω_L and $\omega_L + \Delta\omega_L$, and a bias field $B_0\hat{y}$ produces a Zeeman shift $\hbar\omega_Z = g\mu_B B_0 \approx \hbar\Delta\omega_L$ [see Figs. 1(a) and 1(b)]. Since the momentum transfer is along \hat{x} , the single-particle Hamiltonian can be written as $\mathcal{H} = \mathcal{H}_1(k_x) + [\hbar^2(k_y^2 + k_z^2)/2m + V(\vec{r})] \otimes \mathbf{1}$, where \mathcal{H}_1 is the Hamiltonian for the Raman coupling, the Zeeman energies and the motion along \hat{x} , and $\mathbf{1}$ is the 3×3 unit matrix acting on the spins. $V(\vec{r})$ is the state-independent trapping potential (arising from a far-off-resonance dipole trap and the scalar light shift of the Raman beams), and m is the atomic mass. In the rotating wave approximation for the frame rotating at $\Delta\omega_L$, \mathcal{H}_1/\hbar expressed in the state basis of the family $\Psi(\tilde{k}_x)$ is

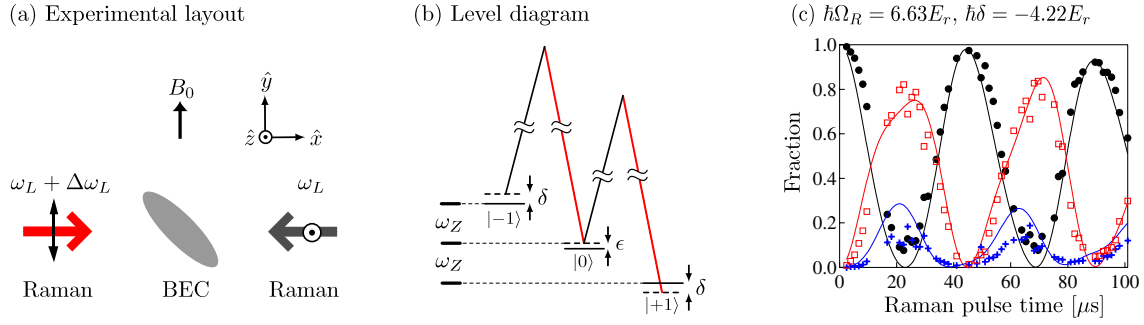


FIG. 1 (color online). (a) The ^{87}Rb BEC in a dipole trap created by two 1550 nm crossed beams in a bias field $B_0\hat{y}$ (gravity is along $-\hat{z}$). The two Raman laser beams are counterpropagating along \hat{x} , with frequencies ω_L and $(\omega_L + \Delta\omega_L)$, linearly polarized along \hat{z} and \hat{y} , respectively. (b) Level diagram of Raman coupling within the $F = 1$ ground state. The linear and quadratic Zeeman shifts are ω_Z and ϵ , and δ is the Raman detuning. (c) As a function of Raman pulse time, we show the fraction of atoms in $|m_F = -1, k_x = 0\rangle$ (solid circles), $|0, -2k_r\rangle$ (open squares), and $|+1, -4k_r\rangle$ (crosses), the states comprising the $\Psi(\tilde{k}_x = -2k_r)$ family. The atoms start in $| -1, k_x = 0\rangle$, and are nearly resonant for the $| -1, 0\rangle \rightarrow |0, -2k_r\rangle$ transition at $\hbar\delta = -4.22E_r$. We determine $\hbar\Omega_R = 6.63(4)E_r$ by a global fit (solid lines) to the populations in $\Psi(-2k_r)$.

$$\begin{pmatrix} \frac{\hbar}{2m}(\tilde{k}_x + 2k_r)^2 - \delta & \Omega_R/2 & 0 \\ \Omega_R/2 & \frac{\hbar}{2m}\tilde{k}_x^2 - \epsilon & \Omega_R/2 \\ 0 & \Omega_R/2 & \frac{\hbar}{2m}(\tilde{k}_x - 2k_r)^2 + \delta \end{pmatrix}.$$

Here $\delta = (\Delta\omega_L - \omega_Z)$ is the detuning from Raman resonance, Ω_R is the resonant Raman Rabi frequency, and ϵ accounts for a small quadratic Zeeman shift [Fig. 1(b)]. For each \tilde{k}_x , diagonalizing \mathcal{H}_1 gives three energy eigenvalues $E_j(\tilde{k}_x)$ ($j = 1, 2, 3$). For dressed atoms in state j , $E_j(\tilde{k}_x)$ is the effective dispersion relation, which depends on experimental parameters, δ , Ω_R , and ϵ (left panels of Fig. 2). The number of energy minima (from one to three) and their positions \tilde{k}_{\min} are thus experimentally tunable. Around each \tilde{k}_{\min} , the dispersion can be expanded as $E(\tilde{k}_x) \approx \hbar^2(\tilde{k}_x - \tilde{k}_{\min})^2/2m^*$, where m^* is an effective mass. In this expansion, we identify \tilde{k}_{\min} with the light-induced vector gauge potential, in analogy to the Hamiltonian for a particle of charge q in the usual magnetic vector potential \vec{A} : $(\vec{p} - q\vec{A})^2/2m$. In our experiment, we load a trapped BEC into the lowest energy, $j = 1$, dressed state, and measure its quasimomentum, equal to $\hbar\tilde{k}_{\min}$ for adiabatic loading.

Our experiment starts with a 3D ^{87}Rb BEC in a combined magnetic-quadrupole plus optical trap [12]. We transfer the atoms to a crossed dipole trap, formed by two 1550 nm beams, which are aligned along \hat{x} - \hat{y} (horizontal beam) and $\sim 10^\circ$ from \hat{z} (vertical beam). A uniform bias field along \hat{y} gives a linear Zeeman shift $\omega_Z/2\pi \approx 3.25$ MHz and a quadratic shift $\epsilon/2\pi = 1.55$ kHz. The BEC has $N \approx 2.5 \times 10^5$ atoms in $|m_F = -1, k_x = 0\rangle$, with trap frequencies of ≈ 30 Hz parallel to, and ≈ 95 Hz perpendicular to the horizontal beam.

To Raman couple states differing in m_F by ± 1 , the $\lambda = 804.3$ nm Raman beams are linearly polarized along \hat{y} and \hat{z} , corresponding to π and σ relative to the quantization axis \hat{y} . The beams have $1/e^2$ radii of $180(20)$ μm [13], larger than the 20 μm BEC. These beams give a scalar light shift up to $60E_r$, where $E_r = h \times 3.55$ kHz, and

contribute an additional harmonic potential with frequency up to 50 Hz along \hat{y} and \hat{z} . The differential light shift between adjacent m_F states arising from the combination of misalignment and imperfect polarization is estimated to be smaller than $0.2E_r$. We determine Ω_R by observing population oscillations driven by the Raman beams and fitting to the expected behavior [Fig. 1(c)].

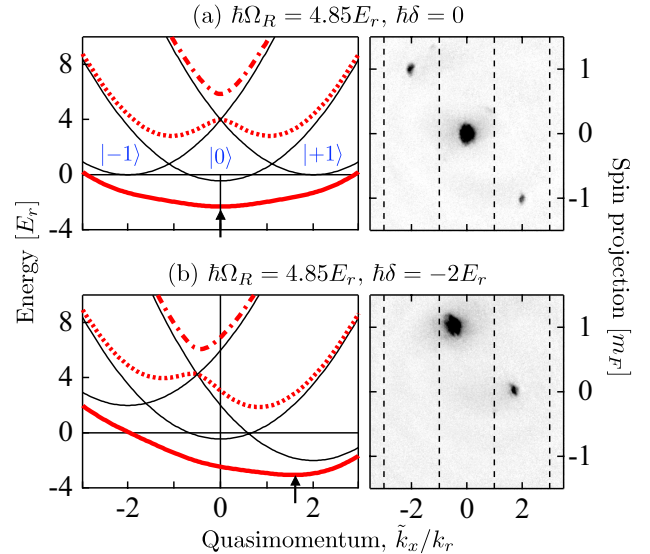


FIG. 2 (color online). Left panels: Energy-momentum dispersion curves $E(\tilde{k}_x)$ for $\hbar\epsilon = 0.44E_r$ and detuning $\hbar\delta = 0$ in (a) and $\hbar\delta = -2E_r$ in (b). The thin solid curves denote the states $| -1, \tilde{k}_x + 2k_r\rangle$, $|0, \tilde{k}_x\rangle$, $|+1, \tilde{k}_x - 2k_r\rangle$ absent Raman coupling; the thick solid, dotted and dash-dotted curves indicate dressed states at Raman coupling $\hbar\Omega_R = 4.85E_r$. The arrows indicate $\tilde{k}_x = \tilde{k}_{\min}$ in the $j = 1$ dressed state. Right panels: Time-of-flight images of the Raman-dressed state at $\hbar\Omega_R = 4.85(35)E_r$, for $\hbar\delta = 0$ in (a) and $\hbar\delta = -2E_r$ in (b). The Raman beams are along \hat{x} , and the three spin and momentum components, $| -1, \tilde{k}_{\min} + 2k_r\rangle$, $|0, \tilde{k}_{\min}\rangle$, and $|+1, \tilde{k}_{\min} - 2k_r\rangle$, are separated along \hat{y} (after a small shear in the image realigning the Stern-Gerlach gradient direction along \hat{y}).

We developed a procedure to adiabatically load the BEC initially in $|-1, k_x = 0\rangle$ to the lowest energy, $j = 1$, Raman-dressed state. For a BEC initially in $|0, k_x = 0\rangle$, this could be achieved simply by slowly turning on the Raman beams at $\delta = 0$, resulting in the $j = 1$, $\tilde{k}_x = 0$ dressed state, located at the minimum of $E_{j=1}(\tilde{k}_x)$. However, our initial state $|-1, k_x = 0\rangle$, for which $k_x = \tilde{k}_x + 2k_r$, is a member of the family $\Psi(\tilde{k}_x = -2k_r)$. This loading procedure would therefore result in the $j = 1$, $\tilde{k}_x = -2k_r$ dressed state. To transfer our $\tilde{k}_x = -2k_r$ BEC to the desired $\tilde{k}_x = 0$ dressed state, we use an additional rf coupling which mixes families with \tilde{k}_x differing by $2k_r$. The rf frequency is equal to the frequency difference between two Raman beams, $\Delta\omega_L/2\pi = 3.250$ MHz. The loading sequence is as follows: (i) We turn on the rf coupling in 1 ms to a resonant Rabi frequency $\Omega_{\text{rf}}/2\pi = 12$ kHz, with an initial detuning $\hbar\delta = 15E_r$. We then sweep the detuning to resonance [14] in 9 ms (δ is varied by ramping the bias field B_0 , leaving $\Delta\omega_L$ constant), loading the atoms into the lowest energy rf-dressed state, a spin superposition still at $k_x = 0$. (ii) We ramp on the Raman coupling in $t_{\text{on}} = 20$ ms to a variable Rabi frequency Ω_R , and then turn off the rf in 2 ms. This loads the BEC into the $j = 1$, $\tilde{k}_x = 0$ dressed state, where it heats at ~ 0.3 nK/ms, likely due to technical noise in B_0 or $\Delta\omega_L$. Therefore, in step (ii) we further evaporatively cool by decreasing the intensity of the horizontal trapping beam by 20% in 20 ms, after which it remains constant. The evaporation reduces the BEC number to $\approx 7 \times 10^4$.

In the final step (iii), we load the $\tilde{k}_x = 0$ dressed state into a nonzero \tilde{k}_x state by sweeping the detuning from resonance to a variable δ in t_{sw} and holding for t_h . As we will show, this adiabatically loads the BEC into the $j = 1$ Raman-dressed state at $\tilde{k}_x = \tilde{k}_{\text{min}}(\delta)$ for $t_{\text{sw}} \geq 20$ ms.

We characterize the Raman-dressed state by abruptly turning off the dipole trap and the Raman beams in less than $1 \mu\text{s}$, projecting the atomic state onto its individual spin and momentum components. The atoms then expand in a magnetic field gradient applied during time-of-flight (TOF) approximately along \hat{y} , and the three spin states spatially separate due to the Stern-Gerlach effect. Imaging the atoms after a 20 ms TOF gives the momentum and spin composition of the dressed state (see right panels of Fig. 2). The quasimomentum $\hbar\tilde{k}_x$ is given by the shift along \hat{x} of all three spin components from their positions when $\tilde{k}_x = 0$. We determine $\tilde{k}_x = 0$ to within $0.03 k_r$ by using the loading procedure above, except that in (ii), the Raman frequencies are sufficiently far-detuned that the atoms experience the scalar light shift but are not Raman-coupled; then the rf and Raman fields are snapped off concurrently before TOF.

It is easy to adiabatically load into the rf-dressed state in step (i) because the smallest relevant energy gap is the $\hbar\Omega_{\text{rf}}/\sqrt{2}$ separation between rf-dressed states. The associated time scale of $\approx 20 \mu\text{s}$ is much less than the 1 ms

turn-on time and the 9 ms ramp time and step (i) is easily adiabatic. To confirm subsequent adiabatic loading from the rf-dressed state into the Raman-dressed state in step (ii), we ramped up the Raman power in a time t_{on} , then ramped it off in t_{on} . Here the energy gap between dressed states at $\tilde{k}_x = 0$ is greater than $\hbar\Omega_{\text{rf}}/\sqrt{2}$ (the added Raman coupling increases the gap). We observe no discernible excitation into other dressed states for $t_{\text{on}} \geq 2$ ms, justifying the loading time $t_{\text{on}} = 20$ ms in step (ii). To determine t_{sw} in step (iii), we measure \tilde{k}_x as a function of t_{sw} for negligible t_h . Figure 3 shows \tilde{k}_x versus t_{sw} at $\hbar\delta = 0, 1, 2E_r$ and $\hbar\Omega_R = 5E_r$, for $t_h = 0.1$ ms. We use $t_{\text{sw}} = 20$ ms, the time at which \tilde{k}_x has nearly reached its equilibrium value. This adiabatic following is enabled by the small $\approx h \times 70$ Hz energy gap provided by the external trap, and the time scale observed for adiabatic loading is comparable to our trapping periods. We also modeled this using a 2D finite-temperature mean-field theory [15] and found the same time scale. After t_{sw} , we add a hold time $t_h = 20$ ms during which residual excitations damp.

Figure 2 shows spin-resolved TOF images of adiabatically loaded Raman-dressed states at $\hbar\Omega_R = 4.85(35)E_r$ for $\hbar\delta = -2$ and $0E_r$. The resonance condition, $\delta = 0$, is determined from the symmetry of the rf-dressed state [16], with an uncertainty of $h \times 1.5$ kHz $= 0.4E_r$, limited by the stability of B_0 . The quasimomentum $\hbar\tilde{k}_x = \hbar\tilde{k}_{\text{min}}$, measured as a function of δ , is shown in Fig. 4(a), along with the calculated $\tilde{k}_{\text{min}}(\delta)$. Each different \tilde{k}_{min} represents a spatially uniform vector gauge potential, where $\tilde{k}_{\text{min}} = q\vec{A}/\hbar$ is analogous to the magnetic vector potential with a magnetic field $\vec{B} = \vec{\nabla} \times \vec{A} = \vec{0}$.

For Rabi frequency $\Omega_R \leq 4.47E_r/\hbar$, $E_{j=1}(\tilde{k}_x)$ has multiple minima for some detunings δ . Figure 4(b) shows such multiple \tilde{k}_{min} , expected for $\delta_a < |\delta| < \delta_b$, where $\hbar\delta_a = 0.35(20)E_r$ and $\hbar\delta_b = 1.2(1)E_r$, at $\hbar\Omega_R = 2.95(35)E_r$. At

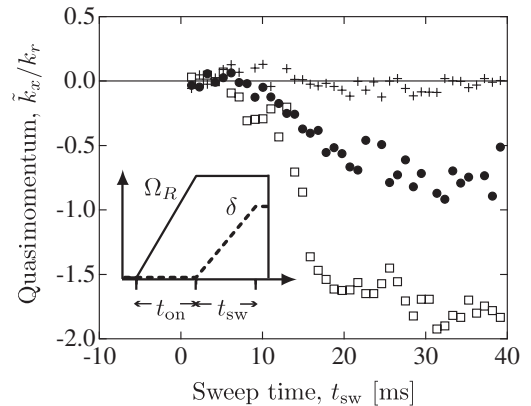


FIG. 3. Quasimomentum $\hbar\tilde{k}_x$ of the Raman-dressed state versus sweeping time t_{sw} of Raman detuning from $\hbar\delta = 0$ to $\hbar\delta = 1E_r$ (solid circles) and $\hbar\delta = 2E_r$ (open squares), at $\hbar\Omega_R = 5E_r$. The crosses denote $\tilde{k}_x = 0$ without sweeping ($\hbar\delta = 0$). The inset shows the time sequence of Ω_R and δ for the loading into a detuned Raman-dressed state.

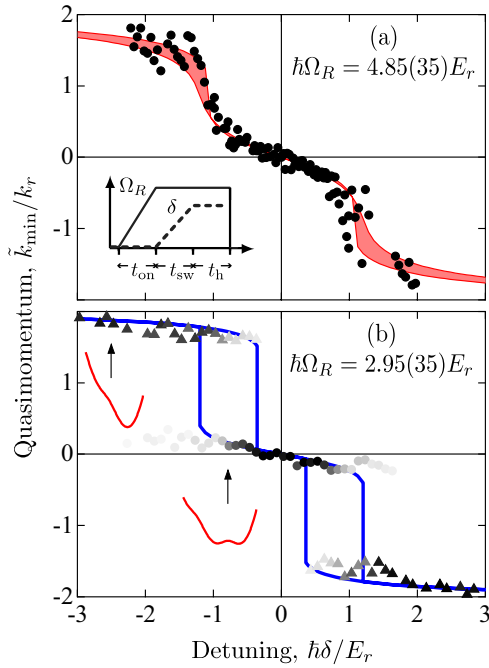


FIG. 4 (color online). (a) Measured quasimomentum $\hbar\tilde{k}_{\min}$ versus detuning δ , and the calculated $\hbar\tilde{k}_{\min}$ at Raman coupling $\hbar\Omega_R = 4.85(35)E_r$ (with the uncertainty indicated by the shaded region). The inset shows the time sequence of Ω_R and δ . (b) Quasimomentum $\hbar\tilde{k}_{\min 1}$ (circles) and $\hbar\tilde{k}_{\min 2}$ (triangles) versus detuning δ , and the calculated $\hbar\tilde{k}_{\min}$ (solid lines) at $\hbar\Omega_R = 2.95(35)E_r$. The intensity of the circles indicates the population of $|0, \tilde{k}_{\min 1}\rangle$ relative to its value at $\delta = 0$. The intensity of the triangles for $\delta < 0$ ($\delta > 0$) indicates the population of $|+1, \tilde{k}_{\min 2} - 2k_r\rangle$ ($|-1, \tilde{k}_{\min 2} + 2k_r\rangle$) relative to its value at $\hbar\delta = -3E_r$ ($\hbar\delta = 3E_r$). The insets picture $E(\tilde{k}_x)$ at $\hbar\delta = -0.8$ and $-2.5E_r$, as indicated by the arrows.

small and large detuning, we observe only one \tilde{k}_{\min} . However, at intermediate detuning, we observe two \tilde{k}_{\min} at $\tilde{k}_{\min 1}$ and $\tilde{k}_{\min 2}$ [11]. In Fig. 4(b), the relative population is indicated by the gray scale, and the solid line is the calculated value(s). The observed $\tilde{k}_{\min}(\delta)$ agrees well with the theory, and a simultaneous fit of $\tilde{k}_{\min 1}$ and $\tilde{k}_{\min 2}$ with Ω_R as a free parameter gives $\hbar\Omega_R = 2.9(3)E_r$, which agrees well with the independently measured $\hbar\Omega_R = 2.95(35)E_r$. As expected, we observe population in only one \tilde{k}_x for $|\delta| < \delta_a$, however, for some $|\delta| > \delta_b$, there is discernible population in two \tilde{k}_x where we expect only one \tilde{k}_{\min} . We attribute this to nonadiabaticity when $\tilde{k}_{\min 1}$ disappears during the detuning sweep in loading step (iii).

In conclusion, we have prepared a Bose-Einstein condensate in a Raman-dressed state with a nonzero quasimomentum, controlled by the Rabi frequency Ω_R and the detuning δ . This technique, in conjunction with a spatial gradient of the bias field (and therefore the detuning) along \hat{y} , would give a spatial gradient of light-induced momentum $\hbar\tilde{k}_{\min}(y)\hat{x}$ and would create an effective magnetic field along \hat{z} [17]. Using an easily tunable magnetic field gradient to create the effective magnetic field is likely a

technical simplification compared with proposals which rely on spatial variations in the light-fields [8]. The analog of the magnetic length $l_B = \sqrt{\hbar/(qB)}$ is $(\partial\tilde{k}_{\min}/\partial y)^{-1/2}$, and is about the spacing between vortices in a vortex lattice like that formed in a rotating BEC [5]. For a gradient in \tilde{k}_{\min} of k_r across a condensate of radius R , this gives an analog $l_B \approx 1.4 \mu\text{m}$ for a $R \approx 10 \mu\text{m}$ 3D BEC, and we expect a ~ 25 -vortex lattice to form in the condensate. For dilute 2D systems, this is sufficient to reach the quantum Hall regime.

This work was partially supported by ONR, ODNI, ARO with funds from the DARPA OLE program, and the NSF through the JQI Physics Frontier Center. R. L. C. acknowledges support from NIST-NRC.

*ian.spielman@nist.gov

- [1] B. Paredes *et al.*, Nature (London) **429**, 277 (2004); T. Kinoshita, T. Wenger, and D. Weiss, Science **305**, 1125 (2004).
- [2] M. Greiner *et al.*, Nature (London) **415**, 39 (2002); T. Stöferle *et al.*, Phys. Rev. Lett. **92**, 130403 (2004); I. B. Spielman, W. D. Phillips, and J. V. Porto, Phys. Rev. Lett. **98**, 080404 (2007).
- [3] D. C. Tsui, H. L. Stormer, and A. C. Gossard, Phys. Rev. Lett. **48**, 1559 (1982); R. B. Laughlin, Phys. Rev. Lett. **50**, 1395 (1983).
- [4] J. R. Abo-Shaeer, C. Raman, J. M. Vogels, and W. Ketterle, Science **292**, 476 (2001); V. Bretin, S. Stock, Y. Seurin, and J. Dalibard, Phys. Rev. Lett. **92**, 050403 (2004).
- [5] V. Schweikhard *et al.*, Phys. Rev. Lett. **92**, 040404 (2004).
- [6] I. Bloch, J. Dalibard, and W. Zwerger, Rev. Mod. Phys. **80**, 885 (2008).
- [7] D. Jaksch and P. Zoller, New J. Phys. **5**, 56 (2003); A. S. Sørensen, E. Demler, and M. D. Lukin, Phys. Rev. Lett. **94**, 086803 (2005); M. Hafezi, A. S. Sørensen, E. Demler, and M. D. Lukin, Phys. Rev. A **76**, 023613 (2007).
- [8] G. Juzeliūnas and P. Öhberg, Phys. Rev. Lett. **93**, 033602 (2004); G. Juzeliūnas, J. Ruseckas, P. Öhberg, and M. Fleischhauer, Phys. Rev. A **73**, 025602 (2006).
- [9] S.-L. Zhu *et al.*, Phys. Rev. Lett. **97**, 240401 (2006).
- [10] J. Higbie and D. M. Stamper-Kurn, Phys. Rev. Lett. **88**, 090401 (2002); F. Papoff, F. Mauri, and E. Arimondo, J. Opt. Soc. Am. B **9**, 321 (1992).
- [11] T. D. Stanescu, B. Anderson, and V. Galitski, Phys. Rev. A **78**, 023616 (2008).
- [12] Y.-J. Lin *et al.* (to be published).
- [13] Uncertainties reflect the uncorrelated combination of 1σ statistical and systematic uncertainties.
- [14] All the detuning ramps are linear versus time, and the Raman beam power turns on nearly quadratically.
- [15] P. B. Blakie *et al.*, Adv. Phys. **57**, 363 (2008).
- [16] On resonance the rf-dressed state has equal population in $|-1, k_x = 0\rangle$ and $|+1, k_x = 0\rangle$, even for a nonzero ϵ . $\delta = 0$ determined from the symmetry of the Raman dressing is within $0.25E_r$ of that from the rf-dressed states.
- [17] I. B. Spielman (to be published).